Effect of hydrogen on methane conversion to hydrocarbons in "one-step" reaction under non-oxidative conditions at low temperature over Pd–Co/SiO_2 catalysts prepared by the sol/gel method

L. Guczi [a,*], L. Borkó [a], Zs. Koppány [a] and F. Mizukami [b]

[a] *Department of Surface Chemistry and Catalysis, Institute of Isotope and Surface Chemistry, Chemical Research Center, Hungarian Academy of Sciences, PO Box 77, Budapest H-1525, Hungary*

[b] *Department of Surface Chemistry, National Institute of Materials and Chemical Research, Tsukuba, Ibaraki 305, Japan*

Received 7 April 1998; accepted 10 June 1998

Methane conversion to higher hydrocarbons in a "one-step" process under non-oxidative conditions at low temperature was here first introduced and investigated over Co–Pd/SiO_2 catalysts at 250 °C as a function of hydrogen concentration in helium and of catalyst composition. A maximum in the production of C_{2+} hydrocarbons including aromatics (benzene and toluene) was observed at 1.3 vol% H_2/He mixture in which one pulse of methane was introduced. Additional hydrogenation with the same H_2/He mixture at 400 °C was efficient to remove the larger hydrocarbon fragments already existing on the surface. On pure Pd/SiO_2 the one-step process is not so efficient as on cobalt-rich samples, but in the latter case the hydrocarbon removal is the most efficient during high-temperature hydrogenation. It was found that methane conversion in the one-step process is at least 2.5 times greater than that measured in the "two-step" process and, in some cases, 80% of the methane introduced is converted to larger hydrocarbons. The results are discussed in terms of the hydrogen coverage ensuring the optimum hydrogen content in the surface CH_x species leading to chain growth.

Keywords: Co–Pd/SiO_2 catalysts, preparation by sol/gel method, one-step methane conversion, hydrogen and composition effect

1. Introduction

There are three broad areas in which methane conversion to form larger hydrocarbons under non-oxidative conditions is considered: (i) two-step reaction [1–3], (ii) methane to aromatics [4–8], and (iii) heterolytic C–H bond cleavage in methane to form aromatics in the presence of carbenium ions using Ga/MFI [9–11]. The last two reactions are quite specific in aromatic formation, while in the first one a wide range of hydrocarbons can be produced, but with a lower conversion.

Since the discovery of the two-step reaction in the non-oxidative, low-temperature methane conversion over metal catalysts, such as Pt, Co and Ru, it has been fully accepted that in the first step methane is chemisorbed to produce CH_x surface species followed by hydrogenation of the CH_x species to form hydrocarbons [12–15]. The yield, i.e., the fraction of the surface CH_x species converted into higher hydrocarbons, depends on the metal itself [3], the structure and morphology of the metal particles [16] and the support [17,18]. The conversion, i.e., the fraction of methane introduced and converted into larger hydrocarbons is normally low, although in some cases the yield amounts to 100%.

In the previous studies carried out on Pt–Co/NaY [12] and Co–Ru/NaY [14] catalysts it was established that the nano-scale bimetallic particles encapsulated into the zeolite supercages, revealed high activity in C–H bond rupture in methane and the platinum and ruthenium components of the bimetallic particles facilitated dissociation of the hydrogen molecules active in removing the surface species. In absence of hydrogen, some experiments carried out under UHV conditions have already indicated formation of the C_2 units during methane chemisorption [18,19]. Those experiments, however, were performed in a static system and the local hydrogen concentration increased during the C–H bond cleavage in methane. On the other hand, we have not received information whether or not larger hydrocarbons are formed during methane chemisorption under flow system [20]. Nevertheless, indirect evidences are available about the surface conversion process during methane impact, such as change in the hydrogen flow rate [20] and the effect of helium treatment [21].

Here we wish to find more details about the scenario of the surface processes, i.e., we wish to know whether CH_x species start polymerizing during methane chemisorption and the hydrogen helps only in removing the hydrogen-deficient carbon species, or the CH_x species starts polymerizing *only during hydrogenation*. Methane chemisorption is principally an endotherm process [22] and the quasi-equilibrium is shifted to more and more hydrogen-deficient surface CH_x species as, e.g., the hydrogen flow rate is altered or the temperature increases. Beyond a threshold value in the number of hydrogen atoms of the surface CH_x

---

[*] To whom correspondence should be addressed.

species, CH_x becomes inactive in the surface chain-growing process. Since the hydrogen is continuously removed from the surface during the methane flow, the system is starving in hydrogen. Since the optimum value of x is about 2 in the surface CH_x species (it depends on the metal [13], the support [17] and, in some cases, on the pretreatment conditions), when methane is chemisorbed in the presence of hydrogen, the x value in the CH_x species is ensured to be higher than without hydrogen, making it more capable for polymerization. This is the idea of the one-step process, and, under this condition, we assume that surface polymerization of the C_1 units starts already during chemisorption.

In the present work, pulse experiments and temperature-programmed reaction are used to study the one-step conversion of methane. The catalysts are prepared by sol/gel technique and have been characterized by XPS [23].

2. Experimental

2.1. Catalyst preparation

The palladium and cobalt samples, denoted as 1R and 5R, contain only cobalt and only palladium (1R and 5R, respectively), and 2R to 4R cobalt and palladium in various atomic ratios (Pd/Co for 2R, 3R and 4R are 1 : 2, 1 : 1 and 2 : 1, respectively). The total metal loading is 5 wt%. Sample 5R was prepared in the following way. Dinitro-diamminepalladium, $Pd(NO_2)_2(NH_3)_2$ (0.002 mol), was dissolved in 22 g of ethyleneglycol containing acetylacetone, $CH_3COCH_2COCH_3$ (0.016 mol), at 80 °C. After stirring for 10 min, 14.8 g of tetraethylorthosilicate, $Si(OC_2H_5)_4$, was added to the solution and mixed at 80 °C for 2 h to give a homogeneous reddish transparent solution. To the reddish transparent solution, 5.12 g of water was added and stirred at 80 °C for 8 h to give a transparent gel. The gel was dried at 80 °C under reduced pressure, powdered and activated in a hydrogen stream of 6 l/h at 400 °C for 4 h. For the preparation of the samples 2R–4R, before the addition of $Si(OC_2H_5)_4$, the ethanol solution of cobalt nitrate hexahydrate $Co(NO_3)_3{\cdot}6H_2O$ was added to the ethyleneglycol solution containing $Pd(NO_2)_2(NH_3)_2$ and $CH_3COCH_2COCH_3$. The procedures after this are the same as described above. The sample 1R was prepared by adding first the ethanol solution of $Co(NO_3)_3{\cdot}6H_2O$ to ethyleneglycol and mixing it with $Si(OC_2H_5)_4$. The residual procedures are the same as in the case of 5R. Here, acetylacetone was not used, because sample 1R does not contain Pd, that is, it is not necessary to stabilize Pd complex in order to prevent the deposition of Pd black. The characterization of the samples was carried out by means of XRD.

2.2. Sample characterizations

The samples were characterized by temperature-programmed reduction (TPR) using 1 vol% hydrogen/argon mixture with $20\,^{\circ}C\,min^{-1}$ ramp rate. An apparatus Sorbstar equipped with quadrupole mass spectrometer type Hiden HAL 02/100 was employed for the TPR measurements. As the samples were already reduced at 400 °C for 4 h, the post-reduction TPR gives information only about the composition of the outer skin of the catalyst grains.

X-ray diffraction (XRD) data were collected by a Mac Science model MPX 18 powder X-ray diffractometer. The palladium particle size was calculated on the basis of Pd(111) or Pd(200) faces.

X-ray photoelectron spectroscopy (XPS) of the samples was performed on the reduced catalyst samples using an XSAM-800 cpi photoelectron spectrometer manufactured by Kratos. Al K_α and Mg K_α characteristic X-ray lines were applied using a 80 eV pass energy for measuring cobalt and palladium spectra, respectively. The use of two different sources was necessary, because for cobalt, the oxygen Auger peak is overlapping the Co 2p binding energy region when the Mg K_α source is employed. On the other hand, when Al K_α is applied for measuring the palladium peak, the cross talk is disturbing. An *in situ* cell was used for the post-treatment of the catalyst samples [23]. Thus, it was possible to measure the surface composition of palladium and cobalt as well as the valence state of the component in the samples in the as-received state, after reduction at 400 °C for 2 h, after oxidation at 300 °C for 2 h and, finally, after second reduction at 400 °C for 2 h. In calculation, the Si 2p was used as a reference (103.3 eV binding energy). The details have been published elsewhere [23] and here only the results are used.

2.3. Catalytic reaction

The reaction for methane conversion was investigated in a flow system detailed elsewhere [7] using 100 mg catalyst in the temperature range between 150 and 250 °C. After post-reduction in a stream of hydrogen at 250 °C, one $0.5\ cm^3$ ($22.3\ \mu l$) methane pulse (in some cases 10 pulses) was introduced into the system into a stream of helium or in a mixture of H_2/He (1.3–75 vol% hydrogen) with a total flow rate of $100\ cm^3\,min^{-1}$ at various temperatures. The reaction products were collected in a trap at liquid-nitrogen temperature and, after warming up, they were analyzed by means of a gas chromatograph type Chrompack CP 9002 using a 50 m long plot fused silica column (0.53 mm I.D.) with a stationary phase of CP-Al_2O_3/KCl with a temperature-programmed mode. After having the samples analyzed, the catalyst was heated in a stream of hydrogen/helium mixture to 400 °C and then, at this temperature, the sample was hydrogenated for 1 h and the products were again collected in a cold trap and were analyzed as previously. The unconverted methane was not trapped at liquid-nitrogen temperature because no zeolite filling was used. The reaction was characterized by the amount of C_{2+} products in μmol (in methane equivalents) and related to the amount of catalyst, or the rate was calculated in $\mu mol\,s^{-1}\,g_{cat}^{-1}$ by calculating the contact time from the flow rate and the volume of the methane pulse. Selectivity was calculated by $(C_i/C_{2+}) \times 100$, $i = 1$–8.

Table 1
CO and H_2 chemisorption data and Pd particle size measured over Co–Pd/SiO_2.

Catalyst	Pd content (μmol/g_{cat})	H_2 (ads) (μmol/g_{cat})	CO (ads) (μmol/g_{cat})	Pd particle size (XRD) (nm) Pd(111)	Pd particle size (XRD) (nm) Pd(200)	Dispersion (%) XRD[a]	Dispersion (%) H_2	Dispersion (%) CO
Co100	–	–	12.8	–	–	–	–	–
Co67	225	–	4.9	4.6	–	24.3	–	2.2
Co50	301	11	8.5	6.1	6.1	18.3/18.3	4.6	2.8
Co33	367	6.3	14	8.5	5.8	13.1/19.3	3.4	3.8
Co0	470	6.7	13	16	13.1	7/8.5	2.8	2.8

[a] The two values represent the dispersion calculated from the average diameter from Pd(111) and Pd(200) reflections, respectively.

3. Results and discussion

3.1. Hydrogen and CO chemisorption

In a paper published earlier [23], we established that the cobalt–palladium samples reduced after preparation at 400 °C for 4 h, followed by passivation on exposing it to air at room temperature, still must be reduced using a 1 vol% H_2/Ar mixture. Hydrogen and carbon monoxide were used in pulse mode to determine the metal surface exposed. In table 1 the results are presented. The results based upon the chemisorption data may give an estimation of the particle size, because stoichiometry of the adsorption is not available. The dispersion of the palladium particles determined from the hydrogen and carbon monoxide chemisorption are presented in the last two columns in table 1 assuming a $H/Pd = 1$ and $CO/Pd = 1$ stoichiometry, respectively.

3.2. X-ray diffraction measurements

The catalysts were investigated by XRD and the data are shown in table 1. The palladium particle size of the various palladium-containing samples are presented using the Pd(111) and Pd(200) reflections. From the average particles size of palladium, d_{av}, presented in columns 5 and 6, the dispersion, which is displayed in column 7, can be calculated for the various Co–Pd/SiO_2 samples. The two dispersion values calculated from XRD and chemisorption significantly deviate from each other, which will be discussed later.

3.3. Temperature-programmed reaction (TPRE) of CH_4 over $Pd_{67}Co_{33}/SiO_2$ sample

1 vol% H_2/Ar as carrier gas was applied, in which 15 and 100 μl methane was pulsed over 105 mg catalyst sample previously reduced in a stream of hydrogen at 400 °C for 1 h. The products were collected in a cold trap filled with zeolite 5A (Supelco) and cooled to liquid-nitrogen temperature. In the temperature-programmed mode, 25 pulses of methane (100 μl each, total 100 μmol) were introduced to the catalyst and, when the trap was warmed up, the products collected were measured by QMS. Only ethane and propane were observed, which were formed in about 1% quantity, as shown in figure 1. As no such products are formed in absence of hydrogen, consequently, the presence of 1 vol% H_2/Ar mixture was sufficient to promote the polymerization of the surface CH_x species formed from methane. When TPRE was applied up to 500 °C temperature (see figure 2) using 100 μl CH_4 pulses (4 μmol each) in 1 vol% H_2/Ar without liquid-nitrogen trap, up to 450 °C neither methane, nor products (ethane and propane) were observed indicating that methane (intensity of the peak at $m/e = 16$) was retained by the catalyst. A significant increase in the QMS signals starts around 500 °C, at which temperature the spikes characteristic of non-reacted methane are superimposed to the broad enveloping curves which are indicative of the desorption of methane and the products (ethane at $m/e = 30$ and propane at $m/e = 29$).

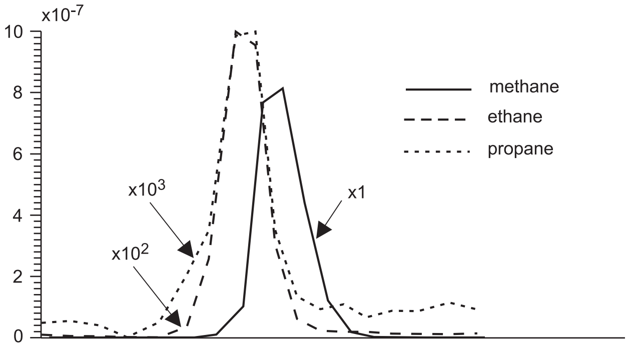

Figure 1. The products formed over the $Co_{67}Pd_{33}/SiO_2$ sample in temperature-programmed reaction mode in the temperature range 25–300 °C after introduction of thirty 15 μl pulses of methane (0.6 μmol each). The mixture is trapped in zeolite 5A, cooled at −196 °C and, after warming up, analyzed with a mass spectrometer.

3.4. One-step methane conversion to larger hydrocarbons

In the first series of experiments using a plug flow reactor, 100 mg $Pd_{67}Co_{33}/SiO_2$ sample was employed and the effect of hydrogen partial pressure in the H_2/He mixture with a total flow rate of 100 $cm^3\,min^{-1}$ was measured. At 250 °C, 10 successive pulses of methane (22.3 μmol each) were introduced and the hydrogen concentration was altered from 0 to 80 vol%. The products formed (in μmol/100 mg catalyst) vs. hydrogen vol% are plotted in figure 3, and, at 1.3 vol%, H_2/He a maximum is observed. The selectivity of C_2 fraction also shows a maximum at the same hydrogen composition. The effect of hydrogen concentration on the selectivity of the reaction products vs. hydrogen concentration is shown in table 2. The scenario of the hydrogen effect is quite obvious: the higher the olefin fraction, the higher the amount of aromatic compounds, and conversely, the amount of olefins depends on the amount of hydrogen in helium.

Our experiments on Pt–Co/NaY [12] and Ru–Co/NaY [14] systems pursued earlier indicated some deactivation of the catalysts on introducing successive pulses. Experiments were carried out in the present work to find out more about the deactivation effect in the following way. Each pulse introduced was trapped at liquid-nitrogen temperature, then the cooled trap was warmed up, and the products were analyzed by gas chromatograph. During this procedure, which lasted for about one hour, 1.3 vol% H_2/He mixture was flown through the catalyst sample at the reaction temperature. Having finished the analysis, the second pulse was added and the procedure in the first step was repeated. The result is presented in table 3. As appears from columns 11 and 12, the amount of the products expressed in μmol/100 mg catalyst as well as the rate of C_{2+} formation decrease with increasing number of pulses. This is indicative of the deactivation of the $Pd_{67}Co_{33}/SiO_2$sample; hence, we changed our strategy and, from now on, always fresh samples were applied and only one pulse of methane was used at 250 °C to study the one-step conversion of methane. The deactivation might decrease at higher temperature.

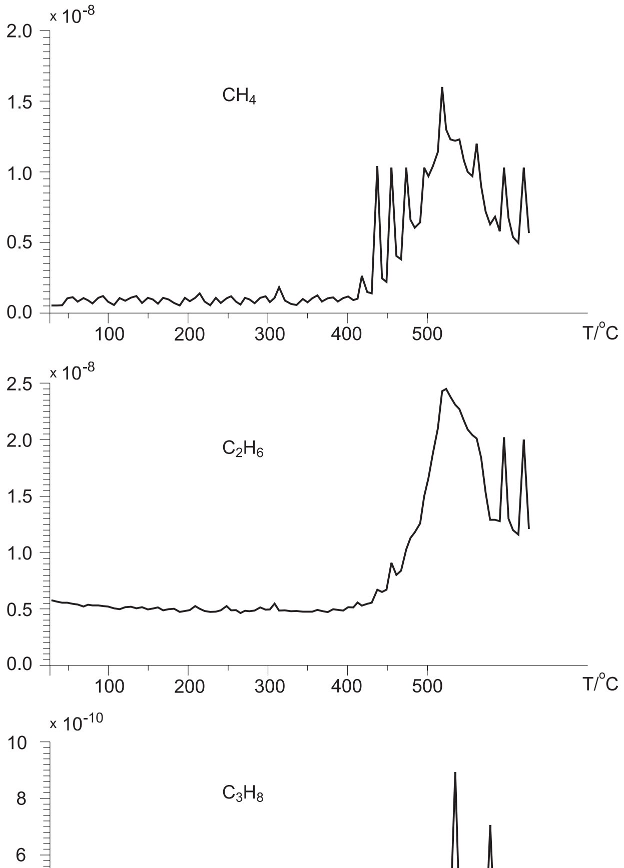

Figure 2. Temperature-programmed reaction (TPRE) of methane over the $Co_{67}Pd_{33}/SiO_2$ sample. The conditions are the same as in figure 1. The amount of methane introduced is 100 μl (4 μmol each) without liquid-nitrogen trap. The final temperature is 500 °C.

3.5. *Comparison of the one- and two-step methane conversion*

In table 4 a comparison is shown between the classical two-step methane conversion and the one-step process introduced here, when only 1 pulse of methane was added into

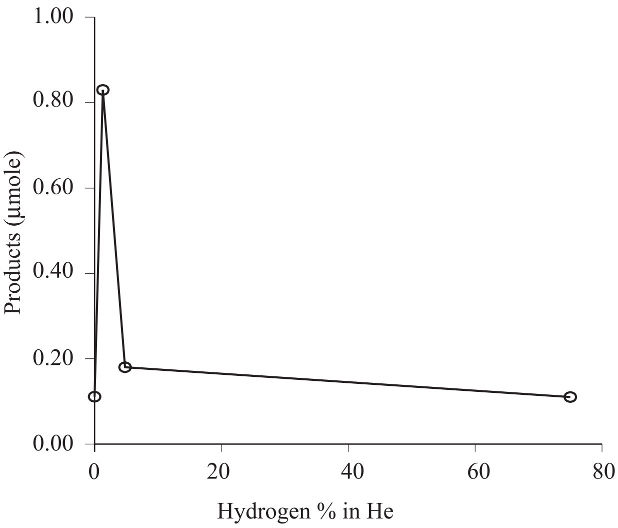

Figure 3. Effect of hydrogen concentration on the C_{2+} products formed over 10 pulses of 0.5 ml (22.3 μmol) methane at 250 °C over 100 mg $Co_{67}Pd_{33}/SiO_2$ sample.

Table 2
Effect of hydrogen on the selectivity of the products formed in one-step methane conversion.[a]

H_2 (vol%)	C_2		C_3		C_4		C_{5+}	Benzene	Toluene
	C_{2-}	$C_{2=}$	C_{3-}	$C_{3=}$	C_{4-}	$C_{4=}$			
0	11.8	0.14	3.00	0.263	2.36	0.28	82.2	17.8	30.60
1.3	41.9	2.26	4.51	0.10	5.27	0.22	45.7	13.4	2.89
4.8	29.2	–	4.77	–	4.79	–	61.1	4.17	3.85
75	8.46	–	3.08	–	3.08	0.141	85.2	1.35	6.56

[a] $T = 250\,^\circ$C; 10 CH_4 pulses (223 μmol); He total flow rate 100 $cm^3\,min^{-1}$; catalyst: 100 mg $Pd_{33}Co_{67}/SiO_2$.
Note: the amount of products is plotted in figure 4.

Table 3
Change of the catalyst activity and selectivity as a function of number of methane pulses.[a]

No. pulses	C_2		C_3		C_4		C_{5+}	Benzene	Toluene	Products	Rate
	C_{2-}	$C_{2=}$	C_{3-}	$C_{3=}$	C_{4-}	$C_{4=}$				(μmol)	(μmol s^{-1} g^{-1})
1	3.25	0.04	0.65	0.017	0.74	0.13	95.20	4.07	7.71	0.86	75.60
2	7.34	0.17	0.80	0.055	0.76	0.06	90.82	3.15	1.74	0.48	42.10
3	18.73	0.44	2.14	0.122	1.92	0.07	76.58	3.45	2.44	0.16	1.42
4	40.84	1.13	5.70	0.513	4.44	0.49	53.11	7.56	3.59	0.05	0.46

[a] $T = 250\,^\circ$C; 22.3 μmol CH_4 pulse; 1.3 vol% H_2/He; total flow rate 100 cm^3 min^{-1}; catalyst: 100 mg $Pd_{33}Co_{67}/SiO_2$.

Table 4
Comparison of one- and two-step reaction in methane conversion over 100 mg $Pd_{67}Co_{33}/SiO_2$ in 1.3 vol% H_2/He at 250 °C.

Methods	Products (μmol/100 mg$_{cat}$)	S_{C_2} (%)	$S_{C_{3+}}$ (%)	Conditions
1-step	0.72	5.6	94.4	One CH_4 pulse in 1.3% H_2/He
2-step				
1st step CH_4 (ads.)	0.18	23.4	86.6	One CH_4 pulse at 250 °C in He
2nd step 1.3% H_2/He	0.13	31.0	69.0	at 250 °C
1st + 2nd steps	0.31	–	–	–
3rd step 1.3% H_2/He	4.48	21.7	88.3	at 400 °C

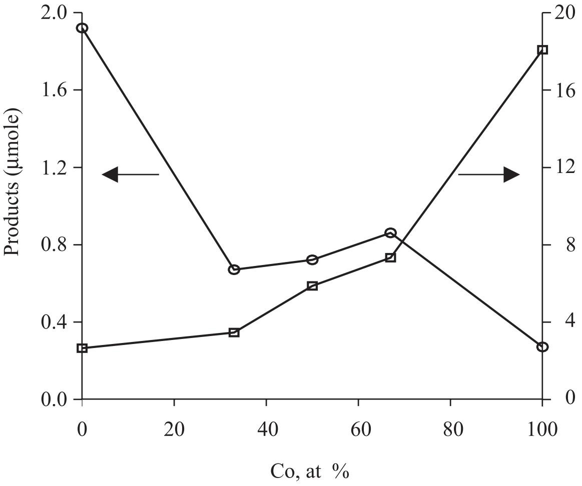

Figure 4. The effect of cobalt concentration in the Co–Pd/SiO_2 samples in one-step methane conversion using one methane pulse (0.5 ml, 22.3 μmol). Left ordinate: amount of C_{2+} products formed at 250 °C over 100 mg catalyst; right ordinate: after subsequent hydrogenation at 400 °C for 1 h.

the gas stream. In the one-step process, 1.3 vol% H_2/He was used as carrier gas like in the 10-pulse experiments, and in the two-step process, the methane was chemisorbed first in pure helium at 250 °C and the hydrogenation was carried out in 1.3 vol% H_2/He mixture as used in the one-step process at the same temperature. In row 1, the products formed in the one-step process are shown and amount to 7.2 μmol/g$_{cat}$, while in the two-step process presented in rows 2 and 3, the amount of products is about 2.5-fold lower. This result undoubtedly demonstrates the advantage of the one-step over the two-step process.

3.6. Effect of catalyst composition on the one-step reaction

The most striking results originated from the amount of products and the selectivity vs. catalyst composition, as shown in figure 4. The amounts of products formed in the one-step methane conversion are high on the pure Pd/SiO_2 sample (5R), constant at the intermediate Pd–Co/SiO_2 catalysts (2R, 3R and 4R), while the pure Co/SiO_2 sample (1R) has the lowest activity. Conversely, after hydrogenation with the 1.3 vol% H_2/He mixture at 400 °C, the amount of products increases in the reversed sequence. That is, by decreasing the palladium content, the catalyst is starving in hydrogen, consequently the surface $(CH_x)_n$ species already present as hydrocarbon chains need hydrogen for removal. This is fully supported when the selectivity of the hydrocarbons formed is considered, as shown in table 5. At 250 °C a fraction of the already polymerized hydrocarbons is still retained by the catalyst surface. By increasing the temperature after the methane in a single pulse has reacted, the amount of products in *hydrogen-assisted desorption* increases and nearly the total amount of methane can be removed from the surface in the form of larger hydrocarbons and as aromatics. This is exclusively possible because the hydrogen in the helium prevents total dehydrogenation of the methane to form fully hydrogen-deficient carbon species as carbonaceous deposits.

In methane interaction with metals the experimental conditions like quality of the carrier gas [20] and flow rate [21], were already found to affect the methane chemisorption. In the latter case, for instance, Bell and coworkers found [20] that the various carbon species on the surface formed from methane can be inter-converted to carbon species with various reactivity. The mass flow rate of hydrogen, which was studied by Amariglio and associates [21], also exerts influence on the methane conversion.

The principle of the one-step reaction we first introduced here is as follows. In previous experiments carried out in our laboratory, cobalt proved to be one of the most efficient metals for metal-based catalysts in methane conversion at low temperature under non-oxidative conditions. However, a metal like cobalt tends to entirely remove the hydrogen atoms from methane and to form completely hydrogen-deficient carbon atoms on the surface which, depending on the temperature, support, particle size, etc., are trans-

Table 5
Effect of catalyst composition on the catalyst activity and selectivity.[a]

Composition	C_2		C_3		C_4		C_{5+}	Benzene	Toluene	Products	Rate
Pd (%)	C_{2-}	$C_{2=}$	C_{3-}	$C_{3=}$	C_{4-}	$C_{4=}$				(μmol)	(μmol s^{-1} g^{-1})
100	1.46	0.04	0.25	0.01	0.22	0.01	98.0	0.52	0.61	1.92	168
77	4.05	3.74	1.37	0.07	1.22	0.11	89.4	4.36	9.21	0.67	59
50	5.64	0.12	0.92	0.10	0.73	0.20	92.3	1.46	2.06	0.72	63
33	3.25	0.04	0.65	0.02	0.74	0.13	95.2	4.07	7.71	0.86	76
0	10.30	4.50	1.20	1.20	0.46	0.81	70.7	2.86	4.30	0.27	24
After hydrogenation with 1.3 vol% H_2/He at 400 °C for 1 h											
100	32.3	0.92	0.26	0.04	0.08	0.04	66.4	39.0	2.94	2.63	–
77	28.1	0.94	0.64	0.13	0.14	0.17	69.9	60.3	2.18	3.44	–
50	17.1	1.45	0.59	0.28	0.27	0.29	80.0	46.6	20.2	5.85	–
33	20.0	2.86	1.30	0.41	0.71	0.65	74.1	46.7	18.5	7.31	–
0	0.94	47.5	0.342	7.22	0.532	5.61	37.9	4.96	3.22	18.10	–

[a] $T = 250\,^\circ C$; 22.3 μmol CH_4 pulse; 1.3 vol% H_2/He; total flow rate 100 $cm^3\,min^{-1}$; catalyst: 100 mg.

formed into non-reactive carbonaceous deposits. These species cannot be reduced and transformed back to higher hydrocarbons. On the other hand, when the metal surface is already partially covered by these non-reactive species, the next incoming methane cannot react so vigorously with the surface, and these hydrogen-containing species become less active in the surface chain-growing process.

Since in methane chemisorption the dissociation of hydrogen atoms from carbon atom increases with temperature, one cannot prevent formation of the fully dehydrogenated carbon, because hydrogen is constantly removed. This is the explanation for the various effects observed and described in the previous paragraph. In order to retard the total dissociation of methane, hydrogen must be admixed to helium to ensure and maintain certain hydrogen coverage on the surface corresponding to the hydrogen partial pressure and temperature. As we have mentioned [13], the optimum performance of a catalyst in the production of larger hydrocarbons, the surface CH_x species with $1 < x \leqslant 2$, must be stabilized. The x value depends on the hydrogen coverage, i.e., if the amount of hydrogen is too high, methane will not chemisorb, or, if so, only in the form of CH_3 species, which is not suitable to build up higher molecular weight hydrocarbons. On the other hand, if hydrogen coverage is zero or very small on the surface, the CH_x species become hydrogen deficient and are unable to polymerize.

This is the explanation for the optimum in the hydrocarbon formation as a function of hydrogen partial pressure in helium. There is, of course, a dedicated balance when the temperature is altered. What is favorable for methane dissociation (e.g., increase in temperature), that is unfavorable for the hydrogen coverage, the latter being decreased with increasing temperature. It looks to us that the conversion of methane related to the amount of methane introduced is higher in the present one-step experiment when we compare it to the two-step runs. Previously, we could measure the efficiency of the conversion of CH_x surface species into larger hydrocarbon molecules, but, even if this surface conversion was 100%, it could not be related to the amount of methane introduced. Although in the present technique a high conversion of methane was measured, the temperature we applied here (250 °C) was not proved to be high enough to remove all the hydrocarbons formed from the surface. The increase of hydrogen concentration proved to be not sufficient, but, raising the temperature to 400 °C, as high as 80% of the methane introduced can be recovered in the form of C_{2+} products. This is very promising for the future methane conversion, because here we can ensure the full recovery, and no oxidation to CO_2 like in the oxidative coupling of methane occurs. The temperature-programmed reaction entirely supports the results.

Now, we have to discuss the structure of the various catalyst composition. The discrepancy between the dispersion calculated from XRD and chemisorption data seems to be ascribed to the cobalt enrichment on the palladium surface. An alternative explanation might result from the preparation method, that is, part of the metal particles could be encapsulated and part of the surface sites are not accessible to hydrogen or CO molecules. The second problem would be that the average size of the particles measured by XRD is always larger (dispersion is smaller) than that measured by chemisorption [24]; however, here the case is reversed.

In previous XPS experiments [23], the Co/Pd ratios on the surface in the bimetallic samples were always over 2, even when the Co/Pd ratio in the bulk was 0.5. The data obtained by XRD indicate a gradual decrease in the average diameter of the palladium particles (see table 1), i.e., an increase in palladium dispersion. Since cobalt cannot be fully reduced (see [23]), the cobalt oxide layer, being interfaced with the silica, may stabilize the smaller palladium particles which are covered by metallic cobalt as the reduction of cobalt interfaced with palladium is facilitated. However, on metallic cobalt the hydrogen is chemisorbed in an activated process [25–28]; thus, only the free palladium sites participate in the hydrogen activation. That is, the dispersion calculated from the number of exposed palladium atoms is smaller than those calculated from XRD data. This gives an explanation why the behaviors of the 2R, 3R and 4R samples are similar (see figure 4) showing the same activities in the methane conversion.

Explanation is required to interpret the large difference between samples 1R and 5R. On Pd/SiO_2 (5R), the amount of products formed in the one-step process is the largest among those observed on the five catalyst samples, but the amount of surface C_{2+} species retained by palladium is very small (after hydrogenation at 400 °C, only minute amount of excess hydrocarbons is formed). That is, the surface chains are weakly bonded. On the other hand, on the Co/SiO_2 sample, most of the C_{2+} species remained strongly bonded to the surface, while at 400 °C, this large portion can be desorbed. This illustrates the high activity of cobalt compared to palladium; however, the recovery of the higher hydrocarbons is hampered on the former sample. The intermediate position in the reactivity of the bimetallic samples shown in figure 4 is due to the cobalt-enriched palladium bimetallic catalysts.

The selectivity values summarized in table 5 indicate a large amount of aromatic formation in the case when large amounts of unsaturated hydrocarbons are produced. This is probably the result of the trimerization of ethylene or dimerization of propene and this mainly occurs on the surface which does not contain enough hydrogen. This clearly appears when the hydrogen concentration is altered (see, e.g., table 2).

4. Conclusions

In the present work, low-temperature, non-oxidative methane conversion in a one-step reaction introduced first here over Co–Pd/SiO_2 samples has been investigated. It was established that:

1. The one-step process carried out at 250 °C is about 2.5-fold more efficient than the two-step counterpart, when 1.3 vol% H_2/He mixture as carrier gas is applied and methane added as pulses;
2. The same result is obtained when the methane conversion occurs in temperature-programmed reaction and 1 vol% H_2/Ar mixture is employed;
3. Additional hydrogenation with the same mixture at 400 °C results in a further recovery of the surface C_{2+} species;
4. The more cobalt is in the bimetallic catalyst, the more C_{2+} species are formed. The catalyst samples are enriched in cobalt as indicated by the results of XRD and chemisorption method;
5. The results are explained by the optimum hydrogen content of the CH_x species produced from methane. In lower amount of hydrogen, the $1 < x \leqslant 2$ value cannot be set, i.e., in low hydrogen coverage the hydrogen-deficient species are not reactive, whereas at high hydrogen concentration the dissociative chemisorption of methane is hampered.

Acknowledgement

The authors are indebted to the COST program (D5/0001/93), to the Japan–Hungarian Exchange Program in Science and Technology (grant No. NP-1826/95-JAP) and to the National Science and Research Fund (grant No. T-022117) for financial support. The sample preparation carried out by Miss M. Ando, XRD measurements made with a Mac Science model MPX 18 are greatly acknowledged.

References

[1] M. Belgued, P. Pareja, A. Amariglio and H. Amariglio, Nature 352 (1991) 789.
[2] T. Koerts, M.J.A. Deelen and R.A. van Santen, J. Catal. 138 (1992) 101.
[3] L. Guczi, R.A. van Santen and K.V. Sarma, Catal. Rev. Sci. Eng. 38 (1996) 329.
[4] Y. Xu, S. Liu, L. Wang, M. Xie and X. Guo, Catal. Lett. 30 (1995) 135.
[5] F. Solymosi, A. Szőke and J. Cserényi, Catal. Lett. 32 (1995) 43.
[6] F. Solymosi, A. Szőke and J. Cserényi, Catal. Lett. 39 (1996) 157.
[7] L. Chen, L. Lin, Z. Xu, T. Zhang and X. Li, Catal. Lett. 39 (1996) 169.
[8] P. Qiu, J.H. Lunsford and M.P. Rosynek, Catal. Lett. 48 (1997) 11.
[9] V.R. Choudary, A.N. Kinage and T.V. Choudary, Science 275 (1997) 1286.
[10] V.R. Choudary, A.N. Kinage and T.V. Choudary, Appl. Catal. A 162 (1997) 239.
[11] V.R. Choudary, A.N. Kinage and T.V. Choudary, Angew. Chem., in press.
[12] L. Guczi, K.V. Sarma and L. Borkó, Catal. Lett. 39 (1996) 43.
[13] L. Guczi, Zs. Koppány, K.V. Sarma, L. Borkó and I. Kiricsi, in: *Progress in Zeolite and Microporous Materials*, Stud. Surf. Sci. Catal., Vol. 105, eds. H. Chon, S.-K. Ihm and Y.S. Uh (Elsevier, Amsterdam, 1997) p. 861.
[14] L. Guczi, K.V. Sarma and L. Borkó, J. Catal. 167 (1997) 495.
[15] M. Belgued, A. Amariglio, L. Lefort, P. Pareja and H. Amariglio, J. Catal. 161 (1996) 282.
[16] L. Guczi, R. Sundararajan, Zs. Koppány, Z. Zsoldos, Z. Schay, S. Niwa and F. Mizukami, J. Catal. 167 (1997) 482.
[17] L. Guczi, K.V. Sarma, Zs. Koppány, R. Sundararajan and Z. Zsoldos, in: *Natural Gas Conversion*, Stud. Surf. Sci. Catal., Vol. 105, eds. M. de Pontes, R.L. Espinosa, C.P. Nicolaides, J.H. Scholz and M.S. Scurrel (Elsevier, Amsterdam, 1997) p. 333.
[18] P. Lenz-Solomun, M.-C. Woo and D.W. Goodman, Catal. Lett. 25 (1994) 75.
[19] Z. Hlavathy, Z. Paál and P. Tétényi, J. Catal. 166 (1997) 118.
[20] S. Monteverdi, A. Amariglio, P. Pareja and H. Amariglio, J. Catal. 172 (1997) 259.
[21] J.N. Carstens and A.T. Bell, J. Catal. 161 (1996) 423.
[22] P. Tétényi, React. Kinet. Catal. Lett. 53 (1994) 369.
[23] L. Guczi, G. Stefler, Z. Schay and F. Mizukami, J. Mol. Catal., in press.
[24] L. Guczi, T. Hoffer and Z. Zsoldos, J. Mol. Catal. 92 (1994) 167.
[25] C.H. Bartholomew, in: *New Trends in CO Activation*, Stud. Surf. Sci. Catal., Vol. 64, ed. L. Guczi (Elsevier, Amsterdam, 1991) p. 187.
[26] Z. Zsoldos, T. Hoffer and L. Guczi, J. Phys. Chem. 95 (1991) 798.
[27] L. Guczi, T. Hoffer, Z. Zsoldos, S. Zyade, G. Maire and F. Garin, J. Phys. Chem. 95 (1991) 802.
[28] Z. Zsoldos and L. Guczi, J. Phys. Chem. 96 (1992) 9393.